Computing the Voronoi Cell of a Lattice: The Diamond-Cutting Algorithm

Emanuele Viterbo and Ezio Biglieri, *Fellow, IEEE*

***Abstract*—Numerical evaluation of some typical lattice parameters such as density, thickness, dimensionless second moment (quantizing constant), etc., are considered. Computational complexity grows exponentially with the dimension of the lattices and all known results rely on the very regular structure of some of these. In this paper we present a general algorithm which enables computation of all the common parameters for any given lattice by means of a complete description of its Voronoi cell. Using this algorithm, we have computed previously unknown values of the quantizing constants of some particularly interesting lattices. These results can be used to evaluate the performance of lattice quantizers and lattice signal constellations for the Gaussian channel. As an application we evaluate a tight upper bound for the error probability of a lattice constellation used for transmission over the additive white Gaussian noise channel.**

***Index Terms*—Lattice, Voronoi region, computational geometry, packing, covering, quantizing constant, lattice constellation, error probability, quantization.**

I. Introduction

THE COMPLETE geometric structure of a lattice can be found from the description of its Voronoi cell. The knowledge of the Voronoi cell solves at once the problem of the computation of relevant lattice parameters such as packing radius, covering radius, kissing number, center density, thickness, normalized second moment (quantizing constant). The error probability of a lattice constellation, used for transmission over the additive white Gaussian noise channel, can also be effectively evaluated by using some of the above parameters.

The Voronoi cell of certain highly symmetric lattices can be determined analytically. According to [1] the Voronoi cell is completely known for the following lattices: A_n, A_n^*, $D_n, D_n^*, (n \geq 2)$ $E_6, E_6^*, E_7, E_7^*, E_8 \cong E_8^*$, Craig's lattice $A_6^{(2)}$, and the 24-dimensional Leech lattice.[1] No result is available for an arbitrary lattice.

In this paper we propose an algorithm which computes the Voronoi cell of a full-rank arbitrary lattice. The exact knowledge of the Voronoi cell (i.e., knowledge of the coordinates of its vertices, edges, etc.) enables one to compute all the lattice parameters within any degree of accuracy. Theoretically, this algorithm evaluates a closed-form solution to all the above lattice problems. In practice, due to finite-precision arithmetics, round-off errors limit the accuracy of the calculations, but comparison with known (closed-form) results indicates that they do not propagate. Hence, the accuracy of the results can be set *a priori* within the range of the computer floating-point precision.

Using this algorithm we have computed some previously unknown values (Table VI) of the quantizing constants for some particularly interesting lattices. As these lattices do not improve upon the best known lattice quantizers, the conjecture about the optimal lattice quantizers being the duals of the densest lattices [12], [1, p. 62], is not disproved.

Due to the exponentially increasing memory requirements we were able to apply the algorithm up to dimensions between 6 and 8 depending on the lattice type. Many of the lattices used in practice as signal constellations are low-dimensional: consequently, they are within the reach of our algorithm.

In the following we assume the reader is familiar with the basic definitions in lattice theory and in most cases we adopt the notations of [1]. Section II reviews the basic geometric definitions needed to describe the diamond-cutting algorithm (Section III). The name of this algorithm comes from its resemblance to the procedure for cutting a raw diamond into a brilliant. In Section IV we show how to compute all the lattice parameters from the Voronoi cell. Finally, Section V summarizes all the results obtained with the diamond-cutting algorithm. Of special interest is Table VI, where we find the previously unknown quantizing constants for the two locally optimal lattice coverings in $\boldsymbol{R}^4$ found by Dickson [16] and for a five-dimensional extreme lattice covering, which belongs to the class introduced by Barnes and Trenerry in [17].

II. Polytopes and Voronoi Regions

In the following we denote by $\boldsymbol{R}^d$ the d-dimensional Euclidean space, while $\boldsymbol{p} = (p_1, p_2, \cdots, p_d)$ represents a vector or a point of $\boldsymbol{R}^d$. Let $||\boldsymbol{p}||$ denote the Euclidean norm of $\boldsymbol{p}$ and $\langle \boldsymbol{p}, \boldsymbol{q} \rangle$ the standard dot product between vectors $\boldsymbol{p}$ and $\boldsymbol{q}$ in $\boldsymbol{R}^d$. With the notation $\alpha\boldsymbol{p}$ (α a real number) we indicate a vector multiplied component-wise by α.

Definition 1: For $0 \leq k \leq d$, a k-flat in $\boldsymbol{R}^d$ is the affine hull (i.e., the set of linear combinations with coefficients adding up to one) of $k+1$ linearly independent points.

A 0-flat is a *point*, a 1-flat is called a *line*, a 2-flat is called a *plane*, and a $(d-1)$-flat, $d > 3$, is called a *hyper-plane*. There is only one d-flat which corresponds to $\boldsymbol{R}^d$ and for convenience we define the empty set as the (-1)-flat. Equivalently, a k-flat

Manuscript received October 2, 1994; revised August 27, 1995. This work was sponsored by CNR under "Progetto finalizzato trasporti."

The authors are with the Dipartimento di Elettronica, Politecnico di Torino I-10129 Torino, Italy.

Publisher Item Identifier S 0018-9448(96)00085-5.

[1] The normalized second moment is computed by Monte Carlo integration using some efficient decoding algorithm of the Leech lattice.

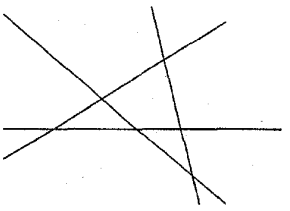

Fig. 1. Example of two-dimensional arrangement of four lines.

can be defined as the intersection of $d-k$ hyper-planes whose normal vectors are linearly independent.

Definition 2: Given a finite set H of hyper-planes in $\boldsymbol{R}^d$ we call arrangement $\mathcal{A}(H)$ of H the dissection of $\boldsymbol{R}^d$ in connected pieces of various dimensions.

The two-dimensional arrangement of Fig. 1 has six intersection points, eight segments, eight half-lines, three bounded regions, and eight unbounded regions.

Definition 3: A (convex) polytope $\mathcal{P}$ is the bounded region defined by the intersection of a finite number of closed half-spaces. More specifically, we call $\mathcal{P}$ a k-polytope if it has dimension k, that is, if k is the smallest integer number such that $\mathcal{P}$ is contained in a k-flat.

In other words, we can say that a polytope is a bounded region delimited by a finite number of hyper-planes. The minimum number of hyper-planes needed to define a k-polytope is $k+1$, since this must be bounded. Any bounded region of an arrangement is a polytope, thus it is possible to adapt to polytopes the algorithms designed for arrangements.

Definition 4: For $0 \leq k \leq d$, a k-face of $\mathcal{P}$ is the set of points of $\mathcal{P}$ contained in a k-flat.

We generally speak of *faces of* $\mathcal{P}$ when k is not specified. The 0-faces are called *vertices of* $\mathcal{P}$, the 1-faces, *edges of* $\mathcal{P}$, and the $(d-1)$-faces, *facets of* $\mathcal{P}$. For convenience we identify $\mathcal{P}$ with the d-face and the empty set with the (-1)-face.

To give a complete description of a polytope we must know all the relations among its faces. For $-1 \leq k \leq d-1$ a k-face f and a $(k+1)$-face g are *incident upon* each other if f belongs to the boundary of g; in this case, f is called a *subface of* g and g a *superface of* f. The d-face represents the whole polytope and is the only superface of all the facets. The (-1)-face has no subfaces and is the only subface of all the vertices.

Definition 5: Let f be a k-face $(k>1)$ of a polytope and let $f_1, f_2, \cdots, f_m (m \geq 2)$ be the subfaces of f. The point

$$p(f) = \frac{1}{m} \sum_{i=1}^{m} p(f_i) \tag{1}$$

is called the *centroid* of f. When f is a vertex, then $p(f) = f$.

The centroid lies always inside f since f is convex. It is important to remark that, in general, this point does not coincide with barycenter (or center of gravity) of the face.[2] The centroid is used to evaluate the Voronoi region while the barycenter is needed when computing its volume and second-order moment. The relation between these two points will be given in (8).

[2]We verified that for all the lattices in Tables I–VI except for Di_{4a}, Di_{4b}, BT_5, I_{5b}, and $A_6^{(2)}$ the centroid and the barycenter of all the k-faces of the Voronoi cell coincide.

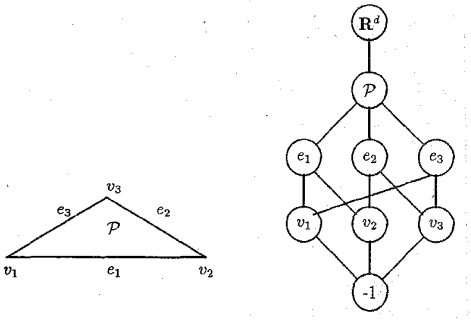

Fig. 2. Example of the incidence graph of the triangle $\mathcal{P}$.

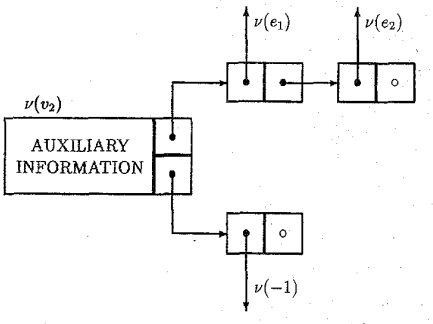

Fig. 3. Data structure of a node. Each node contains the auxiliary information and the pointers to the heads of the superface and subface lists. Each element of the list contains a pointer to a node and a pointer to the next element in the list.

The *incidence graph* $I(\mathcal{P})$ of $\mathcal{P}$ is an undirected graph defined as follows: for each k-face f $(k=-1,0,1,\cdots,d)$ of $\mathcal{P}$, $I(\mathcal{P})$ has a node $\nu(f)$; if f and g are incident upon each other then $\nu(f)$ and $\nu(g)$ are connected by an arc. The incidence graph of a polytope is completed by a node representing the whole Euclidean space $\boldsymbol{R}^d$ which is connected to the d-face (Fig. 2).

In the implementation of the diamond-cutting algorithm, each node $\nu(f)$ of an incidence graph is a record that contains some auxiliary information about the face and two lists containing pointers to the subfaces and the superfaces of f (Fig. 3). The auxiliary information stored in a node consists of the coordinates of the centroid $p(f)$ of f, a component capable of reflecting one of seven colors, the volume of f, the second-order moment of f, the square distance of f from the origin, and a node number.

After these geometric preliminaries we come to the precise definition of Voronoi regions.

Definition 6: Given a discrete set of points Σ in $\boldsymbol{R}^d$ the Voronoi region of a point $\boldsymbol{s}_i \in \Sigma$ is the closed convex set

$$\mathcal{V}(\boldsymbol{s}_i) = \{\boldsymbol{x} \in \boldsymbol{R}^d : \|\boldsymbol{x}-\boldsymbol{s}_i\| \leq \|\boldsymbol{x}-\boldsymbol{s}_j\| \text{ for all } i \neq j\}.$$

In the following we consider sets of points which form lattices. The Voronoi regions of all the lattice points are congruent due to the translation symmetry of the lattice. Hence, we can talk of the Voronoi cell (or region)[3] $\mathcal{V}$ of a

[3]Other names from various fields for the Voronoi cell are *Dirichlet cell, Brillouin zone, Wigner-Seitz cell, Wirk–ungsbereich (domain of action), Wabenzelle (honeycomb), nearest neighbor region, decision region.*

lattice Λ as the Voronoi region around the origin

$$\mathcal{V} = \{\boldsymbol{x} \in \boldsymbol{R}^d : \|\boldsymbol{x}\| \leq \|\boldsymbol{x} - \boldsymbol{u}\| \text{ for all nonzero } \boldsymbol{u} \in \Lambda\}.$$

If $\boldsymbol{u} \neq \boldsymbol{0} \in \Lambda$, then the equation $\|\boldsymbol{x}\| = \|\boldsymbol{x} - \boldsymbol{u}\|$ defines a hyper-plane halfway between $\boldsymbol{0}$ and $\boldsymbol{u}$ ($\langle \boldsymbol{x}, \boldsymbol{u} \rangle = \|\boldsymbol{u}\|^2/2$), and $\|\boldsymbol{x}\| \leq \|\boldsymbol{x} - \boldsymbol{u}\|$ a half-space. $\mathcal{V}$ is an intersection of half-spaces, so it could be a polytope (we must still check if it is bounded). The points $\boldsymbol{p}$ of the lattice for which the hyper-plane between $\boldsymbol{0}$ and $\boldsymbol{p}$ contains a facet of $\mathcal{V}$ are called the *Voronoi-relevant points* and the hyper-planes, *Voronoi-relevant hyper-planes*. If $\boldsymbol{p}$ is Voronoi-relevant also $-\boldsymbol{p}$ is Voronoi-relevant, so $\mathcal{V}$ is symmetric under central (sign) inversion. We say that $\mathcal{V}$ is an $\boldsymbol{0}$-*symmetric convex body*. Since $\mathcal{V}$ cannot contain lattice points $\neq \boldsymbol{0}$, we are under the hypothesis of Minkowski's fundamental theorem [2, p. 25], which implies that $\mathcal{V}$ is bounded. Thus we can conclude that $\mathcal{V}$ is a $\boldsymbol{0}$-symmetric polytope.

Referring to [6] and [7] we also say that $\mathcal{V}$ is a *parallelohedron*, i.e., a *prototile* of a lattice tiling. The Voronoi cell $\mathcal{V}$ is a space-filling parallelohedron with the additional property of being face-to-face, meaning that the intersection of any two distinct tiles is either empty or it is a common k-face for some $k = 0, 1, \cdots, d-1$. Minkowski proved that the maximum number of facets of a d-parallelohedron is $2(2^d - 1)$ [5, pp. 88–96 and pp. 164–169].

Finding the Voronoi region of a lattice is equivalent to determining the Voronoi-relevant points and constructing the polytope bounded by the Voronoi relevant hyper-planes. The Voronoi-relevant points can be found by searching among all the points of the lattice which lie within a sufficiently large bounded region around the origin.

III. The Diamond-Cutting Algorithm

This algorithm computes the incidence graph of the Voronoi region $\mathcal{V}$ of a lattice. From the incidence graph it is possible to extract all the desired lattice parameters as we shall see in the following section. Let us consider a lattice Λ defined by an arbitrary basis $\{\boldsymbol{v}_1, \cdots, \boldsymbol{v}_d\}$. Given a point $\boldsymbol{p}$ we will denote with $h(\boldsymbol{p})$ the hyper-plane passing through the point $\boldsymbol{p}$ and normal to the vector $\boldsymbol{p}$. The distance of $h(\boldsymbol{p})$ from the origin is equal to $\|\boldsymbol{p}\|$. We can now come to the formal description of the algorithm.

Preparation Given the lattice basis $\{\boldsymbol{v}_1, \cdots, \boldsymbol{v}_d\}$ construct the parallelotope $\mathcal{Q}$ defined by the hyper-planes

$$h(\pm\frac{1}{2}\boldsymbol{v}_i), \quad \text{for } i = 1, \ldots, d.$$

$\mathcal{Q}$ contains the Voronoi cell. The corresponding incidence graph $I(\mathcal{Q})$ has 3^d nodes. Finally, set $\mathcal{V} := \mathcal{Q}$.

Cutting Consider all hyper-planes

$$h(\frac{\lambda_1}{2}\boldsymbol{v}_1 + \frac{\lambda_2}{2}\boldsymbol{v}_2 + \cdots \frac{\lambda_d}{2}\boldsymbol{v}_d)$$

with λ_i integers, which cut $\mathcal{V}$ and update $I(\mathcal{V})$ by introducing the nodes corresponding to the new faces and erasing the ones corresponding to the faces which are left out. For this operation we have adapted Edelsbrunner's algorithm for the incrementation of arrangements [3].

Finish Compute $\mathrm{vol}(\mathcal{V})$, the volume of $\mathcal{V}$. If $\mathrm{vol}(\mathcal{V}) > \det(\Lambda)^{1/2}$ go on cutting, else end the algorithm and output the incidence graph $\mathcal{I}(\mathcal{V})$.

We now describe each step of this algorithm in greater detail.

A. Preparation

We first construct the incidence graph of a hypercube with edge length 2 centered at the origin. The $p(f)$ vectors of all the k-faces ($k = 0, 1, \cdots, d$) of this hypercube have components in the set $\{-1, 0, +1\}$. In particular, vertices only have -1 or $+1$ components, edges have one component equal to 0 and the remaining equal to -1 or $+1$, and k-faces have k components equal to 0 and $d - k$ equal to -1 or $+1$. It is now simple to see that a d-dimensional hypercube has $2^{d-k}\binom{d}{k}$ k-faces ($k = 0, 1, \cdots d$) for a total of 3^d faces.

In order to identify the subfaces of a given k-face f it is enough to replace each of the 0 components, in turn, with -1 and $+1$. In this way we find $2k$ subfaces. For the superfaces of f we replace each of the nonzero components, in turn, with a 0, so that we find exactly $d-k$ superfaces. For convenience, these component vectors are considered as base three (digits 0, 1, 2) numbers and then converted to decimal representation. The number is then used as the node number which uniquely identifies a k-face of $\mathcal{Q}$. An example of this is shown in Figs. 4 and 5.

The parallelotope $\mathcal{Q}$, which is only a slanted and stretched hypercube, has the same incidence graph, except for the $p(f)$ vectors. We only need to calculate the vertices coordinates of the parallelotope then, using (1), we recursively obtain all the $p(f)$ vectors of all the faces. The vertices $\boldsymbol{x}^{(m)}, m = 1, \cdots, 2^d$ of $\mathcal{Q}$ are found at the intersection of d hyper-planes

$$\begin{cases} \langle \boldsymbol{v}_1, \boldsymbol{x}^{(m)} \rangle &= \dfrac{\lambda_1^{(m)}}{2}\|\boldsymbol{v}_1\|^2 \\ \langle \boldsymbol{v}_2, \boldsymbol{x}^{(m)} \rangle &= \dfrac{\lambda_2^{(m)}}{2}\|\boldsymbol{v}_2\|^2 \\ \qquad\vdots & \\ \langle \boldsymbol{v}_d, \boldsymbol{x}^{(m)} \rangle &= \dfrac{\lambda_d^{(m)}}{2}\|\boldsymbol{v}_d\|^2 \end{cases} \tag{2}$$

where $\lambda_i^{(m)}$, $i = 1, \cdots, d$ take on the values -1 and $+1$ of the corresponding components of the mth vertex in the hypercube. The solution of all these linear systems is found by inverting once for all the generator matrix of the lattice and multiplying it by the vector of the *known terms*.

B. Cutting

The *raw diamond* is now ready to be cut. Given a hyper-plane $h(\boldsymbol{p})$ cutting $\mathcal{V}$ (i.e., such that $h(\boldsymbol{p}) \bigcap \mathcal{V} \neq \emptyset$) we construct the incidence graph of the two parts of the dissected polytope: the main body and the chip. The main body will always contain the origin since the cutting plane does not

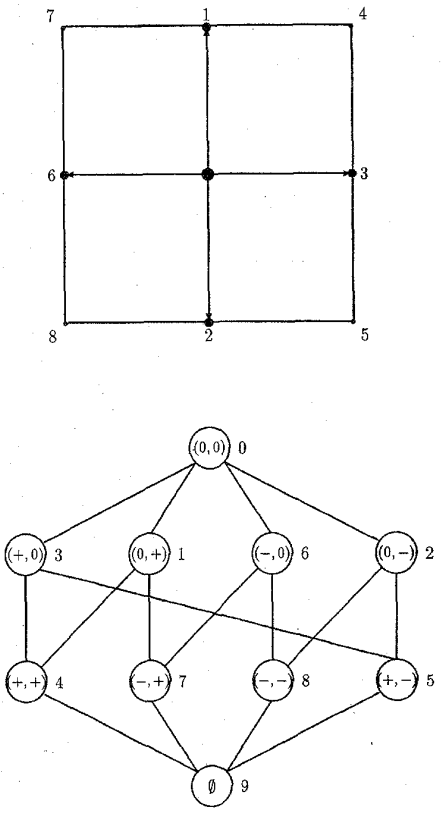

Fig. 4. Incidence graph of a square ("+" stands for +1 and "−" for −1).

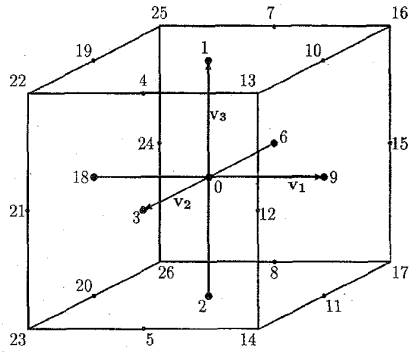

Fig. 5. Node numbers of a cube.

include the origin. This operation is performed by using the color conventions and procedures 7.3-5 described in [3, ch. 7]. Next, the incidence graph is purged of all the nodes representing the chip to obtain the new $\mathcal{I}(\mathcal{V})$.

A key operation in this procedure is to determine whether a given point $\boldsymbol{x}$ lays on, above, or below the cutting hyper-plane. In particular we have

$$\begin{aligned} \langle \boldsymbol{p}, \boldsymbol{x} \rangle &< \|\boldsymbol{p}\|^2 \quad && \boldsymbol{x} \text{ is on the side of the main body} \\ \langle \boldsymbol{p}, \boldsymbol{x} \rangle &= \|\boldsymbol{p}\|^2 \quad && \boldsymbol{x} \in h(\boldsymbol{p}) \\ \langle \boldsymbol{p}, \boldsymbol{x} \rangle &> \|\boldsymbol{p}\|^2 \quad && \boldsymbol{x} \text{ is on the side of the chip.} \end{aligned} \tag{3}$$

This operation uses a fixed tolerance value (e.g., 10^{-5}), given as an input, to resolve the three cases.

Another critical procedure is the search for the coordinates of the new vertices. These are given by the intersections between $h(\boldsymbol{p})$ and the edges of $\mathcal{V}$. A bisection method is used. Starting from a vertex above and a vertex below $h(\boldsymbol{p})$ we compute the midpoint until such a point is found to lie on $h(\boldsymbol{p})$. In this case, the tolerance should be further reduced in order to overcome some ill-conditioned cases which may be encountered when the incidence angle of the edge with the hyper-plane is very small. When this occurs, the midpoint may be very close to the hyper-plane but still quite far from the true intersection point.

C. Finish

Each cut reduces the volume of the polytope. When this is equal to $\det(\Lambda)^{1/2}$, the volume of the *fundamental parallelotope*, we have obtained the Voronoi region of the lattice. In the practical algorithm, the volume is calculated after all the cuts are performed, so the above condition is used to check the consistency of the initial choice of the cutting hyper-planes and the final accuracy of the results.

The way to select all the possible cutting hyper-planes is to consider all the lattice points within a given radius C from the origin by using the algorithm proposed in [4]. A safe choice for such radius would be twice the distance from the origin of the furthest vertex of the initial parallelotope $\mathcal{Q}$. In general, a less conservative choice will work especially when the lattice basis is not reduced [5], [6]. If the covering radius is already known, then this is also a safe value for $C/2$. Whenever C is too small the volume of $\mathcal{V}$ will not reach the value $\det(\Lambda)^{1/2}$, meaning that C should be increased.

IV. Calculating the Lattice Parameters

We now see how to evaluate all the lattice parameters once the incidence graph $\mathcal{I}(\mathcal{V})$ of the Voronoi cell is found.

A. Packing

To calculate the *packing radius* ρ we must find the facet closest to the origin. For this it is sufficient to scan the auxiliary information of the nodes pointed by the subface list of the node $\nu(\mathcal{V})$. At the same time the *kissing number* τ is found (i.e., the number of facets at the packing radius distance from the origin).

The *packing density* Δ is the ratio between the volume of the greatest sphere centered at the origin and contained in $\mathcal{V}$ and the volume of $\mathcal{V}$. This sphere has its radius equal to the packing radius. The *center density* δ is equal to the packing density divided by the volume of the unit sphere.

B. Covering

To calculate the *covering radius* R we must find the vertex of $\mathcal{V}$ with maximum distance from the origin. So it is sufficient to scan the nodes pointed by the superface list of the node $\nu(-1)$.

The *thickness* Θ of a covering of Λ is the ratio between the smallest sphere centered at the origin and containing $\mathcal{V}$ and the volume of $\mathcal{V}$. This sphere has its radius equal to the covering

radius. The *normalized thickness* θ is equal to the thickness divided by the volume of the unit sphere.

C. Quantization Parameters

The *volume* of $\mathcal{V}$ is also given by

$$\text{vol}\,(\mathcal{V}) = \int_{\mathcal{V}} d\boldsymbol{x} \tag{4}$$

and is equal to the volume of the fundamental parallelotope of Λ. The *second-order moment* of $\mathcal{V}$ about $\mathbf{0}$ is defined by

$$U(\mathcal{V}) = \int_{\mathcal{V}} \|\boldsymbol{x}\|^2\, d\boldsymbol{x}. \tag{5}$$

In [1, ch. 21], $\text{vol}\,(\mathcal{V})$ and $U(\mathcal{V})$ are given in terms of the volume $V_{d-1}(i)$ and of the second-order moment of the facets $U_{d-1}(i)$ about the foot of the perpendicular from $\mathbf{0}$, where i runs over the set of facets of $\mathcal{V}$. Let $h_i^{(d-1)}$ be the distance of the facets of $\mathcal{V}$ from the origin. Then

$$\text{vol}\,(\mathcal{V}) = \sum_i \frac{h_i^{(d-1)}}{d} V_{d-1}(i)$$

$$U(\mathcal{V}) = \sum_i \frac{h_i^{(d-1)}}{d+2}\left[h_i^{(d-1)2} V_{d-1}(i) + U_{d-1}(i)\right].$$

These equations cannot be used in our algorithm. In fact, the recursive generalization of these equations, which yield the volume and the second-order moment of a k-face in terms of volume and second-order moment of its subfaces, requires an additional hypothesis which is not satisfied in general for arbitrary lattices. In order to clarify this problem, let $\boldsymbol{c}_i^{(k)}$ be the orthogonal projection of the origin $\mathbf{0}$ on the ith k-face for $k = 2, \cdots, d-1$. We have $h_i^{(d-1)} = \|\boldsymbol{c}_i^{(d-1)}\|$, where i runs over the set of the facets (subfaces) of $\mathcal{V}$. If we consider the mth k-face, then we define

$$h_i^{(k-1)}(m) = \|\boldsymbol{c}_m^{(k)} - \boldsymbol{c}_i^{(k-1)}\|$$

where i runs over the set of all the subfaces of the mth k-face. Due to the orthogonality conditions we have the simple recursion

$$h_i^{(k-1)}(m)^2 = \|\boldsymbol{c}_m^{(k)}\|^2 - \|\boldsymbol{c}_i^{(k-1)}\|^2.$$

The general recursions for $k = 1, \cdots, d$, are

$$V_k(m) = \sum_i \frac{h_i^{(k-1)}(m)}{d} V_{k-1}(i)$$

$$U_k(m) = \sum_i \frac{h_i^{(k-1)}(m)}{d+2}\left[h_i^{(k-1)}(m)^2 V_{k-1}(i) + U_{k-1}(i)\right] \tag{6}$$

with the initial conditions $V_0\,(\text{vertices}) = 1$ and $U_0\,(\text{vertices}) = 0$.

For the validity of these equations it is crucial to assume that the projections $\boldsymbol{c}_m^{(k)}$ of the origin on all the faces falls within them. This is certainly true only for the facets ($k = d-1$) of $\mathcal{V}$ which belong to the Voronoi-relevant hyper-planes and are cut by the normal vector connecting $\mathbf{0}$ to the corresponding Voronoi-relevant point. But in general it is not true for an arbitrary lattice.

We have verified that for all the lattices considered in Section V (6) give the correct results because these lattices are in a sense "special" (highly symmetric). As an example we give the generator matrix of an "arbitrary" lattice for which (6) cannot be applied

$$\begin{pmatrix} 21 & 0 & 0 & 0 \\ 11 & 22 & 0 & 0 \\ 0 & 3 & 23 & 0 \\ 10 & 10 & 10 & 13 \end{pmatrix}.$$

Equations that may be used to calculate recursively $\text{vol}\,(\mathcal{V})$ and $U(\mathcal{V})$ for an arbitrary lattice are derived in the following.

Theorem: With the above notations, let g_m be the mth k-face with barycenter $q(g_m)$, f_i one of its subfaces with barycenter $q(f_i)$. Setting $V_0(vertices) = 1$ and $U_0(vertices) = 0$, for $k = 2, \cdots d$ we have

$$V_k(m) = \sum_i \frac{a_i^{(k-1)}(m)}{d} V_{k-1}(i)$$

$$U_k(m) = \sum_i \frac{a_i^{(k-1)}(m)}{d+2}\left[b_i^{(k-1)}(m)^2 V_{k-1}(i) + U_{k-1}(i)\right] \tag{7}$$

where $a_i^{(k-1)}(m)$ is the distance of $q(g_m)$ from the ith $(k-1)$-face f_i, $b_i^{(k-1)}(m)$ is the distance between $q(g_m)$ and $q(f_i)$, $U_k(m)$ is the second-order moment of the g_m about its barycenter $q(g_m)$, and $U_{k-1}(i)$ is the second-order moment of f_i about its barycenter $q(f_i)$.

Proof: In this case we always have $q(g_m) \in g_m$ and the face g_m can be decomposed into generalized pyramids of vertex $q(g_m)$ and basis f_i. The proof then follows from elementary calculus by slicing each generalized pyramid into slabs parallel to f_i. □

For the use of (7) in the DCA we need to relate the centroid $p(f)$ to the barycenter $q(f)$ of a face f. This is accomplished recursively using the following equation:

$$q(g_m) = \frac{1}{V_k(m)} \sum_i \frac{dq(f_i) + p(g_m)}{d+1} V_k(\mathcal{P}_i), \quad k = 2, \cdots, d \tag{8}$$

where $V_k(\mathcal{P}_i)$ is the volume of the generalized pyramid of vertex $p(g_m)$ and base f_i.[4]

The *dimensionless second moment* or *quantizing constant* of a lattice Λ represents the mean-squared quantization errors per point assuming a uniform input distribution to a lattice quantizer

$$G(\Lambda) = G(\mathcal{V}) = \frac{1}{d} \frac{U(\mathcal{V})}{\text{vol}\,(\mathcal{V})^{1+2/d}}.$$

This value is independent of the scale and the dimension of the space and depends only on the shape of $\mathcal{V}$. For each dimension d, it is lower-bounded by the quantizing constant

[4] An alternative approach, suggested by one of the reviewers, is the insertion into (6) of a "−" sign for the terms where the projection of the origin lies outside the face.

of a d-dimensional sphere with the same volume of $\mathcal{V}$ and radius r.

$$G(\Lambda) \geq \frac{\Gamma\left(\frac{d}{2}+1\right)^{2/d}}{(d+2)\pi}.$$

We also recall that $G(\Lambda)$ is the figure of merit for shaping, when a Voronoi cell is used as a constellation bounding region [8].

D. Error Probability

An upper bound to the error probability $P(e)$ of a finite constellation carved from a lattice and used for transmission over the additive white Gaussian noise channel can be derived as follows. We assume that all the points are transmitted with equal probability and the lattice constellation is sufficiently large to neglect edge effects. Due to the geometric uniformity of the lattice [9] it is enough to consider the probability of decoding a point different from $\mathbf{0}$, when $\mathbf{0}$ is transmitted. Let $\boldsymbol{x}$ be the received vector when $\mathbf{0}$ is transmitted. The components of $\boldsymbol{x}$ are Gaussian distributed random variables, with zero mean and variance σ^2. The exact value of $P(e)$ is then formally written as

$$P(e) = P(\boldsymbol{x} \notin \mathcal{V}) = \frac{1}{(\sqrt{2\pi}\sigma)^d} \int_{\mathcal{V}} \exp\left(-\|\boldsymbol{x}\|^2/2\sigma^2\right) d\boldsymbol{x}.$$

Now let $\boldsymbol{p}_i$ be the Voronoi-relevant points around $\mathbf{0}$. Using the union bound with all the Voronoi-relevant hyper-planes only, we obtain the upper bound [1, p. 70], [11]

$$\begin{aligned} P(e) &\leq P\left(\bigcup_i \left\{\langle \boldsymbol{x}, \boldsymbol{p}_i\rangle \geq \|\boldsymbol{p}_i\|^2/2\right\}\right) \\ &\leq \sum_i P(\langle \boldsymbol{x}, \boldsymbol{p}_i\rangle \geq \|\boldsymbol{p}_i\|^2/2) = \sum_i \frac{1}{2}\operatorname{erfc}\left(\frac{\|\boldsymbol{p}_i\|/2}{\sqrt{2}\sigma}\right). \end{aligned} \tag{9}$$

Bound (9) may be compared with another upper bound given by

$$P(e) < P(\boldsymbol{x} \notin S_\rho) = 1 - \Gamma\left(\frac{d}{2}, \frac{\rho^2}{2\sigma^2}\right) \Big/ \Gamma\left(\frac{d}{2}\right) \tag{10}$$

where S_ρ is a d-dimensional sphere of radius ρ, the packing radius of the lattice, and

$$\Gamma(a,x) = \int_0^x t^{a-1} e^{-t}\, dt$$

is the incomplete gamma function.

A well-known lower bound [10], is given by

$$P(e) > P(\boldsymbol{x} \notin S_{r_0}) = 1 - \Gamma\left(\frac{d}{2}, \frac{r_0^2}{2\sigma^2}\right) \Big/ \Gamma\left(\frac{d}{2}\right) \tag{11}$$

where S_{r_0} is a d-dimensional sphere with volume equal to $\operatorname{vol}(\mathcal{V})$ and radius r_0.

TABLE I
LATTICES A_n

	δ	θ	$G(\mathcal{V})$	N_0	N_1	N_2	N_3	N_4	N_5	N_6	N_7	Total
A_2	0.288676	0.384900	0.080188	6	6							12
A_3	0.176777	0.500000	0.078745	14	24	12						50
A_4	0.111803	0.643990	0.078020	30	70	60	20					180
A_5	0.072170	1.125016	0.077648	62	180	210	120	30				602
A_6	0.047246	1.904147	0.077466	126	434	630	490	210	42			1932
A_7	0.031250	4.000000	0.077396	254	1008	1736	1680	980	336	56		6050
A_8	0.020833	8.128842	0.077391	510	2286	4536	5208	3780	1764	504	72	18660

	$\operatorname{vol}(\mathcal{V})$	Facet profile (ρ^2, τ)		Vertices profile (R^2)	
A_2	1.732043	0.499999	6	0.666664	6
A_3	1.999991	0.499999	12	0.749997	8
				0.999999	6
A_4	2.236056	0.499999	20	0.799997	10
				1.199999	20
A_5	2.449449	0.499999	30	0.833330	12
				1.333325	30
				1.499999	20
A_6	2.645751	0.500000	42	0.857143	14
				1.428571	42
				1.714286	70
A_7	2.828427	0.500000	56	0.875000	16
				1.500000	56
				1.875000	112
				2.000000	70
A_8	3.000000	0.500000	72	0.888889	18
				1.555556	72
				2.000000	168
				2.222222	252

V. RESULTS

In this section we show some of the results obtained with the Diamond-Cutting Algorithm. The algorithm was implemented in standard C and was run on different computers: PC 486, VAX 6000-530, and different UNIX workstations. The best performance in terms of speed was obtained on the workstations.

The major difficulties arise when dimension increases. In fact, the amount of memory required may become very high. Using double-precision arithmetic it was estimated that the system needs to allocate, on average, 170 bytes for each node of the incidence graph. The total memory needed to store the final Voronoi cell can be estimated by looking at the total number of nodes (last column of tables). We specify "final" because during the cutting step the incidence graph of the chip as well as that of the main body must be created. For example, in the case of E_7 the total memory occupied by the Voronoi cell was about 9 MB, while during the cutting operation the peak size of the allocated memory was about 17 MB.

The program receives as input the space dimension, the full-rank lattice generator matrix, and the tolerance parameter which is used to resolve the position of a point with respect to a hyper-plane. This last parameter must be consistent with the accuracy to which the generator matrix is given and approximately determines the final accuracy of the computed parameters. The values in Tables I–VI were obtained with a tolerance value of 10^{-5}. We report the results with six decimal digits to show the numerical stability of the algorithm with respect to this parameter.

In all cases where the lattices are defined by their Gram matrix A, Cholesky decomposition was applied to A, giving $A = LL^T$, with L lower triangular. The matrix L can then be used as a generator matrix of the lattice. If the lattices are defined by a nonfull-rank generator matrix, the Gram matrix is calculated first.

Each lattice appears in two tables. The first one shows all the lattice parameters which are independent of the particular scaling factor, as well as the number N_k of k-faces of the

TABLE II
DUAL LATTICES A_n^*

	δ	θ	$G(\mathcal{V})$	N_0	N_1	N_2	N_3	N_4	N_5	Total
A_2^*	0.288676	0.384900	0.080188	6	6					12
A_3^*	0.162380	0.349385	0.078543	24	36	14				74
A_4^*	0.089444	0.357770	0.077559	120	240	150	30			540
A_5^*	0.048526	0.403566	0.076922	720	1800	1560	540	62		4682
A_6^*	0.026033	0.493668	0.076490	5040	15120	16800	8400	1806	126	47292

	vol($\mathcal{V}$)	Facet profile (ρ^2, τ)		Vertices profile (R^2)	
A_2^*	1.732043	**0.499999**	**6**	**0.666664**	6
A_3^*	3.999995	**0.750000**	**8**	1.249997	24
		0.999991	6		
A_4^*	11.18038	**1.000012**	**10**	**2.000000**	120
		1.499994	20		
A_5^*	36.00000	**1.250000**	**12**	**2.916667**	720
		2.000000	30		
		2.250000	20		
A_6^*	129.6418	**1.500000**	**14**	**4.000000**	5040
		2.500000	42		
		3.000000	70		

TABLE III
LATTICES D_n

	δ	θ	$G(\mathcal{V})$	N_0	N_1	N_2	N_3	N_4	N_5	N_6	N_7	Total
D_2	0.250000	0.500000	0.083333	4	4							8
D_3	0.176777	0.500000	0.078745	14	24	12						50
D_4	0.125000	0.500000	0.076603	24	96	96	24					240
D_5	0.088388	0.873464	0.075786	42	240	400	240	40				2092
D_6	0.062500	1.687501	0.075591	76	576	1200	1120	480	60			3512
D_7	0.044194	3.544893	0.075686	142	1344	3360	3920	2520	840	84		12210
D_8	0.031250	8.000000	0.075914	272	3072	8960	12544	10080	4928	1344	112	41312

	vol($\mathcal{V}$)	Facet profile (ρ^2, τ)		Vertices profile (R^2)	
D_2	8.000000	**2.000000**	**4**	**4.000000**	4
D_3	16.00000	**2.000000**	**12**	3.000000	8
				4.000000	6
D_4	32.00001	**2.000000**	**24**	**4.000000**	24
D_5	64.00000	**2.000000**	**40**	4.000000	10
				5.000000	32
D_6	127.9999	**2.000000**	**60**	4.000000	12
				6.000000	64
D_7	256.0000	**2.000000**	**84**	4.000000	14
				7.000000	128
D_8	512.0000	**2.000000**	**112**	4.000000	16
				8.000000	256

TABLE IV
DUAL LATTICES D_n^*

	δ	θ	$G(\mathcal{V})$	N_0	N_1	N_2	N_3	N_4	N_5	N_6	Total
D_2^*	0.250000	0.500000	0.083333	4	4						8
D_3^*	0.162377	0.349384	0.078543	24	36	14					76
D_4^*	0.125000	0.500000	0.076603	24	96	96	24				240
D_5^*	0.062500	0.474610	0.075625	240	720	720	280	42			2002
D_6^*	0.031250	0.843750	0.075120	160	1440	2880	2160	636	76		7352
D_7^*	0.015625	0.966967	0.074859	2240	10080	17920	15120	6328	1428	142	53258

	vol($\mathcal{V}$)	Facet profile (ρ^2, τ)		Vertices profile (R^2)	
D_2^*	2.000000	**0.500000**	**4**	**1.000000**	4
D_3^*	4.000006	**0.749992**	**8**	**1.249997**	24
		0.999998	6		
D_4^*	8.000000	**1.000000**	**24**	**2.000000**	24
D_5^*	16.00000	**1.000000**	**10**	**2.250001**	240
		1.249999	32		
D_6^*	32.00000	**1.000000**	**12**	**3.000000**	160
		1.500000	64		
D_7^*	63.99999	**1.000000**	**14**	**3.250000**	2240
		1.750000	128		

TABLE V
OTHER LATTICES

	δ	θ	$G(\mathcal{V})$	N_0	N_1	N_2	N_3	N_4	N_5	N_6	Total
$A_6^{(2)}$	0.053995	0.644791	0.075057	798	4368	6944	4452	1176	98		17836
E_6	0.072169	1.368545	0.074347	54	702	2160	2160	720	72		5868
E_6^*	0.064150	0.513201	0.074244	720	6480	10800	6480	1566	126		26172
E_7	0.062500	2.922836	0.073231	632	4788	16128	20160	10080	2016	126	53930
E_7^*	0.045669	0.886223	0.073116	576	10080	40320	50400	23688	4284	182	129530

	vol($\mathcal{V}$)	Facet profile (ρ^2, τ)		Vertices profile (R^2)	
$A_6^{(2)}$	18.520261	**0.999999**	**42**	2.000001	336
		1.500000	56	**2.285715**	462
E_6	1.732037	**0.499998**	**72**	**1.333333**	54
E_6^*	0.577350	**0.333333**	**54**	**0.666667**	720
		0.500000	72		
E_7	16.00000	**1.000000**	**126**	1.750000	576
				3.000000	56
E_7^*	0.707107	**0.375000**	**56**	0.875000	576
		0.500000	126		

TABLE VI
SOME NEW VALUES

	δ	θ	$G(\mathcal{V})$	N_0	N_1	N_2	N_3	N_4	N_5	Total
C_3	0.165779	0.386206	0.078670	24	36	14				74
Di_{4a}	0.113027	0.390822	0.076993	120	240	150	30			540
Di_{4b}	0.076078	0.381728	0.077465	120	240	150	30			540
BT_5	0.035124	0.423672	0.076278	720	1800	1560	540	62		4682
Is_{5a}	0.018042	1.379132	0.084734	48	120	116	54	12		350
Is_{5b}	0.018042	0.848806	0.082839	114	468	600	288	44		1514

	vol($\mathcal{V}$)	Facet profile (ρ^2, τ)		Vertices profile (R^2)	
C_3	2.828427	**0.603553**	**8**	0.957107	8
		0.707107	4	**1.060660**	16
		1.000000	2		
Di_{4a}	2.211152	**0.499998**	**18**	0.904520	90
		0.651365	6	**0.929606**	30
		0.848671	6		
Di_{4b}	5.138604	**0.625246**	**4**	1.375344	60
		0.771980	6	**1.400553**	60
		0.897196	12		
		1.000956	2		
		1.271960	6		
BT_5	170.8081	**2.047607**	**2**	1.375344	60
		2.638084	10	**5.543897**	720
		3.047608	10		
		3.547607	20		
		4.776172	20		
Is_{5a}	9.797850	**0.499997**	**6**	**2.833313**	48
		0.999999	6		
Is_{5b}	9.797875	**0.499998**	**6**	1.999988	48
		0.999999	18	**2.333330**	66
		1.499996	20		

TABLE VII
EXACT VALUES OF CENTER DENSITY, NORMALIZED THICKNESS, AND QUANTIZING CONSTANT FOR THE LATTICES USED FOR COMPARISON
(a is the integer part of $(n+1)/2$ and the values of J_n are given in [1, p. 473]. The first values of J_n are $1/12$, $5/18$, $19/32$, $389/375$, $1045/648$, $78077/33614$ for $n = 1, \cdots, 7$)

Λ	δ	θ	G
$\mathbb{Z}^n$	2^{-n}	$n^{n/2}2^{-n}$	$1/12$
A_n $(n \geq 2)$	$2^{-n/2}(n+1)^{-1/2}$	$\frac{[a(n+1-a)]^{n/2}}{(n+1)^{(n+3)/2}}$	$\frac{1}{(n+1)^{1/n}}\left(\frac{1}{12}+\frac{1}{6(n+1)}\right)$
A_n^* $(n \geq 2)$	$\frac{n^{n/2}}{2^n(n+1)^{(n-1)/2}}$	$\sqrt{n+1}\left(\frac{n(n+2)}{12(n+1)}\right)^{n/2}$	$\frac{J_{n+1}}{n(n+1)^{1-1/n}}$
D_n $(n \geq 3)$	$2^{-(n+2)/2}$	$1/2\,(n=3)$ $n^{n/2}2^{-(n+1)}\,(n \geq 4)$	$\frac{1}{2^{2/n}}\left(\frac{1}{12}+\frac{1}{2n(n+1)}\right)$
D_n^* $(n \geq 5)$	$2^{-(n-1)}$	$n^{n/2}$ (n even) $(2n-1)^{n/2}/2^{2n-1}$ (n odd)	$\frac{2641}{23040\cdot 2^{2/5}} = 0.0756254\,(n=5)$ $\frac{601\cdot 2^{1/3}}{10080} = 0.0751203\,(n=6)$
$A_6^{(2)}$	$\frac{1}{7\sqrt{7}} = 0.05399492$	$\frac{(4/\sqrt{7})^6}{7\sqrt{7}} = 0.64479070$	$\frac{3503}{360\cdot 49\sqrt{7}} = 0.07505723$
E_6	$1/8\sqrt{3}$	$2^6 \cdot 3^{-7/2}$	$\frac{5}{56\cdot 3^{1/6}} = 0.0743467$
E_6^*	$3^{-5/2}$	$2^3 \cdot 3^{-7/2}$	$\frac{12619\cdot 3^{1/6}}{204120} = 0.0742437$
E_7	$1/16$	$3^{7/2} \cdot 2^{-4}$	$\frac{163}{2016\cdot 2^{1/7}} = 0.0732306$
E_7^*	$3^{7/2} \cdot 2^{-10}$	$7^{7/2} \cdot 2^{-10}$	$\frac{21361\cdot 2^{1/7}}{322560} = 0.0731165$

Voronoi cell. The second one gives the parameters which depend on the scaling factor but are still independent of the lattice basis. The column with vol $(\mathcal{V})$ can be compared with the determinant of the generator matrix of the lattice to check the accuracy of the computations. The facets profile gives the number of facets for each square distance. Here we find the squared packing radius and the kissing number (in boldface). The vertices profile gives the number of vertices for each square distance and here we find the square covering radius (in boldface).

Finally, Table VII gives the exact values of δ, θ, and G for the lattices used for testing the accuracy of the algorithm.

Figs. 6–8 show the bounds (9)–(11) for different six-dimensional lattices. Curves of $P(e)$ are plotted as a function of a signal-to-noise ratio defined as

$$\mathrm{SNR}_{\mathrm{dB}} = 10 \log \frac{\sqrt[d/2]{\mathrm{vol}\,(\mathcal{V})}}{4\sigma^2}.$$

$G(\Lambda)$ decreases from Z_6, to A_6, to E_6, and to E_6^*, which indicates that the shape of the Voronoi cell becomes more and more spherical. This is reflected in a smaller gap between the

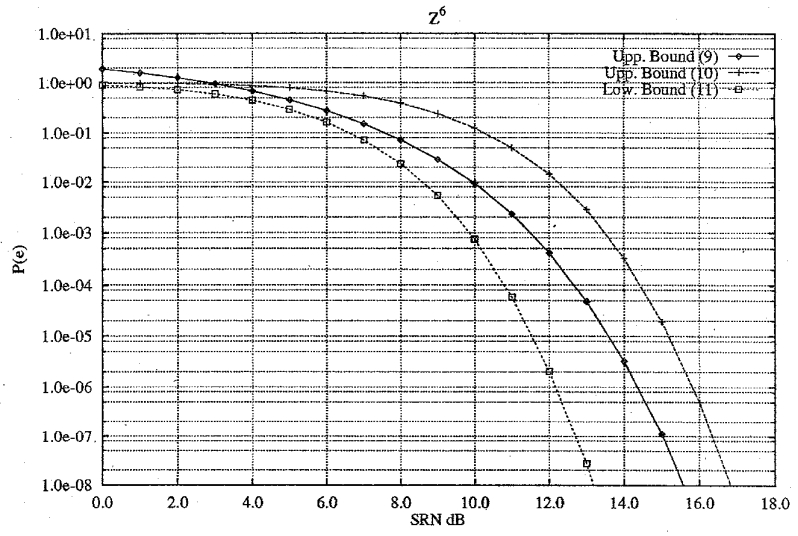

Fig. 6. Upper and lower bounds to point error probability for Z_6.

upper bound (10) and the lower bound (11). The improved union bound (9) comes also very close to the lower bound.

We now list the generator or Gram matrices of the lattices which were tested with the diamond-cutting algorithm. The row vectors of the generator matrices form the lattice basis. Sometimes a scaled version of the lattices was considered.

A. Reference Lattices

For all the lattices in this subsection the Voronoi region is known, so the values of the parameters were used to test the accuracy of the program.

Lattices A_n and A_n^* (Gram matrices) see [1, pp. 108–117]:

$$A_n: \begin{pmatrix} 2 & -1 & 0 & \cdots & 0 & 0 \\ -1 & 2 & -1 & & 0 & 0 \\ 0 & -1 & 2 & & 0 & 0 \\ \vdots & & & \ddots & & \vdots \\ 0 & 0 & 0 & & 2 & -1 \\ 0 & 0 & 0 & \cdots & -1 & 2 \end{pmatrix}$$

$$A_n^*: \begin{pmatrix} n & -1 & -1 & \cdots & -1 & -1 \\ -1 & n & -1 & & -1 & -1 \\ -1 & -1 & n & & -1 & -1 \\ \vdots & & & \ddots & & \vdots \\ -1 & -1 & -1 & & n & -1 \\ -1 & -1 & -1 & \cdots & -1 & n \end{pmatrix}.$$

Lattices D_n and D_n^* (Generator matrices) see [1, pp. 117–120]:

$$D_n: \begin{pmatrix} -2 & -2 & 0 & \cdots & 0 & 0 \\ 2 & -2 & 0 & & 0 & 0 \\ 0 & 2 & -2 & & 0 & 0 \\ \vdots & & & \ddots & & \vdots \\ 0 & 0 & & 2 & -2 & 0 \\ 0 & 0 & 0 & \cdots & 2 & -2 \end{pmatrix}$$

$$D_n^*: \begin{pmatrix} 2 & 0 & 0 & \cdots & 0 & 0 \\ 0 & 2 & 0 & & 0 & 0 \\ 0 & 0 & 2 & & 0 & 0 \\ \vdots & & & \ddots & & \vdots \\ 0 & 0 & 0 & & 2 & 0 \\ 1 & 1 & 1 & \cdots & 1 & 1 \end{pmatrix}.$$

Lattice $A_6^{(2)}$ (Gram matrix): This self-dual lattice is obtained by using Craig's construction [1, p. 223]. Its normalized second moment was computed by Coulson in [12].

$$A_6^{(2)}: \begin{pmatrix} 6 & -4 & 1 & 0 & 0 & 1 \\ -4 & 6 & -4 & 1 & 0 & 0 \\ 1 & -4 & 6 & -4 & 1 & 0 \\ 0 & 1 & -4 & 6 & -4 & 1 \\ 0 & 0 & 1 & -4 & 6 & -4 \\ 1 & 0 & 0 & 1 & -4 & 6 \end{pmatrix}$$

Lattices E_6 and E_6^* (Gram matrices) see [1, pp. 125–127] and [14]:

$$E_6: \begin{pmatrix} 2 & -1 & 0 & 0 & 0 & 0 \\ -1 & 2 & -1 & 0 & 0 & 0 \\ 0 & -1 & 2 & -1 & 0 & -1 \\ 0 & 0 & -1 & 2 & -1 & 0 \\ 0 & 0 & 0 & -1 & 2 & 0 \\ 0 & 0 & -1 & 0 & 0 & 2 \end{pmatrix}$$

$$E_6^*: \begin{pmatrix} 2 & -1 & 0 & 0 & 0 & 0 \\ -1 & 2 & -1 & 0 & -1 & 0 \\ 0 & -1 & 2 & -1 & 0 & -1 \\ 0 & 0 & -1 & 2 & 0 & 0 \\ 0 & -1 & 0 & 0 & 4/3 & 1 \\ 0 & 0 & -1 & 0 & 1 & 2 \end{pmatrix}$$

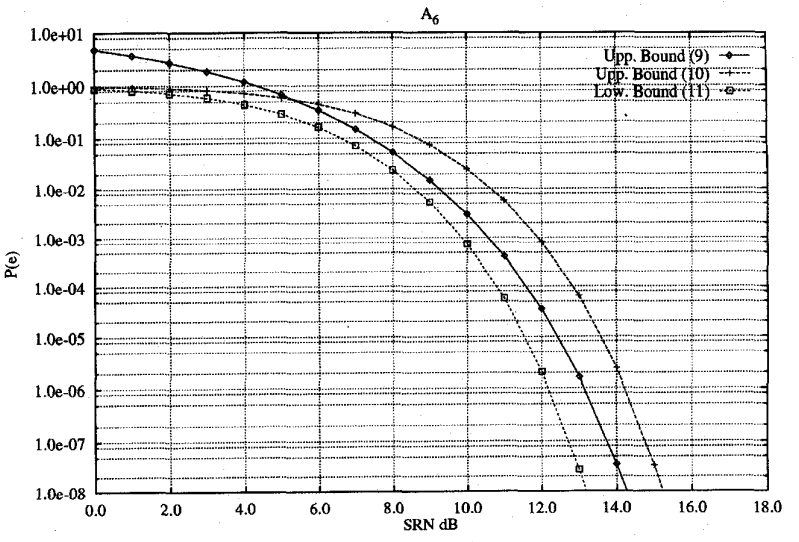

Fig. 7. Upper and lower bounds to point error probability for A_6.

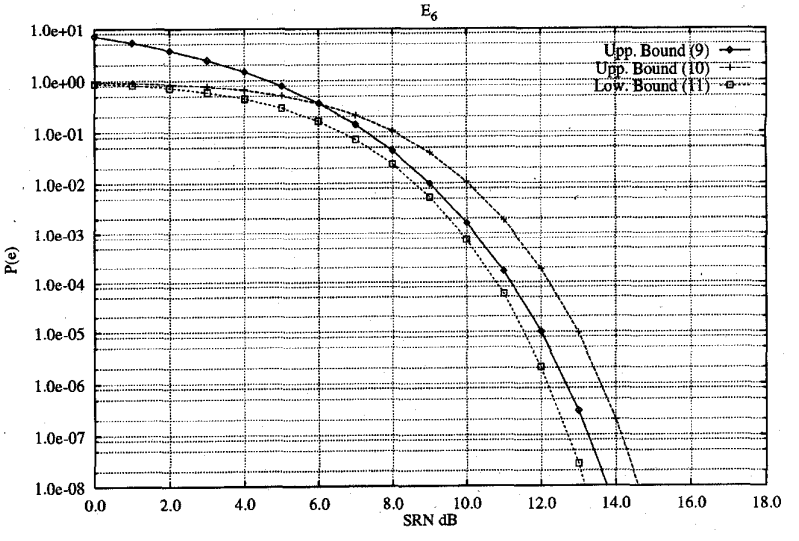

Fig. 8. Upper and lower bounds to point error probability for E_6.

Lattices E_7 (Generator matrix) E_7^* (Gram matrix) see [1, pp. 124–125] and [15]:

$$E_7: \begin{pmatrix} 2 & 0 & 0 & 0 & 0 & 0 & 0 \\ 0 & 2 & 0 & 0 & 0 & 0 & 0 \\ 0 & 0 & 2 & 0 & 0 & 0 & 0 \\ 0 & 0 & 0 & 2 & 0 & 0 & 0 \\ 1 & 1 & 1 & 0 & 1 & 0 & 0 \\ 0 & 1 & 1 & 1 & 0 & 1 & 0 \\ 0 & 0 & 1 & 1 & 1 & 0 & 1 \end{pmatrix}$$

$$E_7^*: \begin{pmatrix} 2 & -1 & 0 & 0 & 0 & 0 & 0 \\ -1 & 2 & -1 & 0 & 0 & 0 & 0 \\ 0 & -1 & 2 & -1 & 0 & 0 & 0 \\ 0 & 0 & -1 & 2 & -1 & 0 & 0 \\ 0 & 0 & 0 & -1 & 2 & -1 & 0 \\ 0 & 0 & 0 & 0 & -1 & 2 & 0 \\ 0 & 1 & 0 & 0 & 0 & 0 & 3/2 \end{pmatrix}$$

B. New Values

The following lattices were considered because they exhibit some interesting feature.

Lattice C_3 (Gram matrix): This lattice was recently proven to be the densest three-dimensional lattice which is geometrically similar to its dual. It is also the thinnest geometrically self-dual covering lattice [1, p. xix]

$$C_3: \begin{pmatrix} 1+\sqrt{2} & 1 & 1 \\ 1 & 1+\sqrt{2} & 1-\sqrt{2} \\ 1 & 1-\sqrt{2} & 1+\sqrt{2} \end{pmatrix}.$$

Lattice Di_{4a} and Di_{4b} (Gram matrices): These two lattices, found by Dickson, together with A_4^* are the three locally optimal lattice coverings in $\boldsymbol{R}^4$ [6]. The values of $G(\Lambda)$, reported in Table VI, answer the question posed in [1, p. 62]: "What is $G(\Lambda)$ for Dickson's four-dimensional lattices (...),

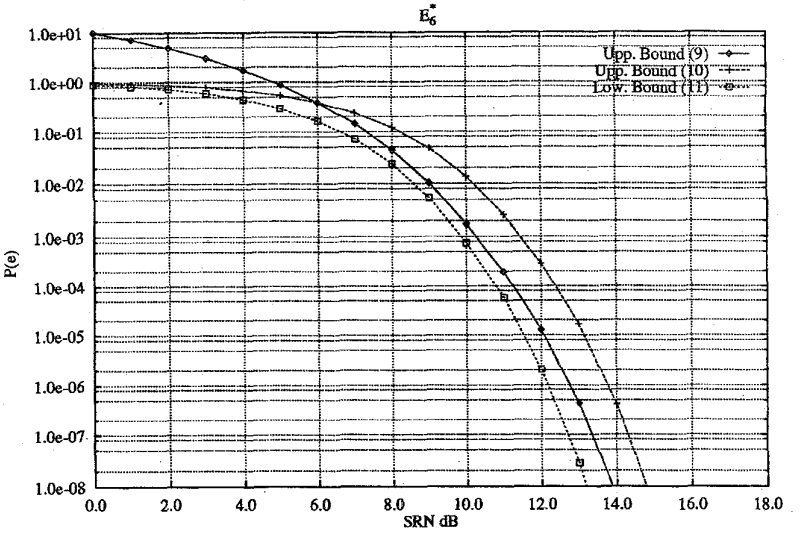

Fig. 9. Upper and lower bounds to point error probability for E_6^*.

or for the Barnes–Trennery lattices (...)?"

$$Di_{4a}: \begin{pmatrix} 2 & \alpha & -1 & -1 \\ \alpha & 2 & -1 & -1 \\ -1 & -1 & 2 & 1-\alpha \\ -1 & -1 & 1-\alpha & 2 \end{pmatrix}$$

$$Di_{4b}: \begin{pmatrix} 3-\gamma & \gamma & -1 & -1 \\ \gamma & 3-\gamma & -1 & -1 \\ -1 & -1 & 2+2\beta & -\beta \\ -1 & -1 & -\beta & 2+2\beta \end{pmatrix}$$

where $\alpha = (5-\sqrt{13})/2$ and $\beta \approx 0.544, \gamma \approx 0.499$ are roots of certain polynomials.

Lattices BT_n (Gram matrices): This family of extreme lattice coverings was given by Barnes and Trenerry in [17]. These lattices exhibit a normalized thickness which is slightly larger than the one of the family of best known lattice coverings A_n^*. This property prompted the question in [1, p. 62] and for $n = 5$ we find that these lattices do not improve over the best known lattice quantizer.

For $n \geq 5$ the Gram matrix is given by

$$BT_n: \begin{pmatrix} 0 & 0 & 0 & 0 & \cdots \\ 0 & n-1 & -1 & -1 & \\ 0 & -1 & n-1 & -1 & \\ 0 & -1 & -1 & n-1 & \\ \vdots & & & & \ddots \end{pmatrix} + \frac{\beta_n}{4} \begin{pmatrix} n & n-2 & -2 & -2 & \cdots \\ n-2 & n & -2 & -2 & \\ -2 & -2 & & & \\ -2 & -2 & & 4I_{n-2} & \\ \vdots & \vdots & & & \end{pmatrix}$$

where I_{n-2} is the $(n-2)$-dimensional identity matrix and β_n is the positive root of

$$3(n-3)x^2 + (n^2-8n-6)x - 4n(n+1) = 0.$$

Lattices Is_{5a} and Is_{5b} (Gram matrices): This is a pair of five-dimensional iso-spectral lattices (i.e., inequivalent lattices with the same theta series); see [1, p. xxi].

$$Is_{5a}: \begin{pmatrix} 2 & 0 & 0 & 2 & 2 \\ 0 & 2 & 0 & 2 & 0 \\ 0 & 0 & 2 & 0 & 2 \\ 2 & 2 & 0 & 8 & 4 \\ 2 & 0 & 2 & 4 & 8 \end{pmatrix} \quad Is_{5b}: \begin{pmatrix} 2 & 1 & 0 & 2 & 2 \\ 1 & 2 & 0 & 2 & 2 \\ 0 & 0 & 6 & 4 & 4 \\ 2 & 2 & 4 & 8 & 4 \\ 2 & 2 & 4 & 4 & 8 \end{pmatrix}$$

VI. Conclusion

In this paper we have presented an algorithm which computes the Voronoi cell of an arbitrary lattice. The knowledge of the Voronoi cell enables one to exactly compute all the relevant lattice parameters. Using the diamond-cutting algorithm we have found some previously unknown values of the quantizing constants of some important lattices.

Most of the computational problems related to lattices are either known or conjectured to be NP-hard [1, p. 40], [18]. The principal limitation in the application of the DCA is the exponentially increasing memory requirement. It is enough to recall that the number of nodes required to describe the fundamental parallelotope is already 3^d. The final number of nodes for the Voronoi cell greatly varies between different lattices in the same dimension. With 32-MB RAM we have reached dimensions between 6 and 8 according to the lattice type. Although we were not able to compute the Voronoi region of the Gosset lattice E_8 due to the memory limitation of our computer, we believe that this problem is within reach of the proposed algorithm. The possibility of reducing the memory requirements appears remote especially if we want to preserve the generality of the algorithm.

Acknowledgment

The authors wish to acknowledge the anonymous referees of the first version of this paper for their comments and

constructive criticism. We are especially grateful to one of them for pointing out an error in the value of the quantizing constant of $A_6^{(2)}$, which was due to our confusion between centroid and barycenter.

REFERENCES

[1] J. H. Conway and N. J. A. Sloane, *Sphere Packings, Lattices and Groups*, 2nd ed. Berlin, Germany: Springer-Verlag, 1992.
[2] P. Erdös, P. M. Gruber, and J. Hammer, *Lattice Points*. Essex, England: Longman, 1989.
[3] H. Edelsbrunner, *Algorithms in Combinatorial Geometry*. Berlin, Germany: Springer-Verlag, 1987.
[4] U. Fincke and M. Pohst, "Improved methods for calculating vectors of short length in a lattice, including a complexity analysis," *Math. Comput.*, vol. 44, pp. 463–471, Apr. 1985.
[5] P. M. Gruber and C. G. Lekkerkerker, *Geometry of Numbers*, 2nd ed. Amsterdam, The Netherlands: North-Holland, 1987.
[6] P. M. Gruber, "Geometry of numbers," in *Handbook of Convex Geometry*, vol. B, P. M. Gruber and J. M. Wills, Eds. Amsterdam, The Netherlands: Elsevier, 1993, pp. 737–764.
[7] E. Schulte, "Tilings," in *Handbook of Convex Geometry*, vol. B, P. M. Gruber and J. M. Wills, Eds. Amsterdam, The Netherlands: Elsevier, 1993, pp. 899–932.
[8] G. D. Forney, "Multidimensional constellations—Part II: Voronoi constellations," *IEEE J. Select. Areas Commun.*, vol. 7, no. 6, pp. 941–958, Aug. 1989.
[9] ——, "Geometrically uniform codes," *IEEE Trans. Inform. Theory*, vol. 37, no. 5, pp. 1241–1260, Sept. 1991.
[10] C. E. Shannon, "Probability of error for optimal codes in a Gaussian channel," *Bell Syst. Tech. J.*, vol. 38, no. 3, May 1959.
[11] E. Biglieri, A. Sandri, and A. Spalvieri, "Computing upper bounds to error probability of coded modulation schemes," in *Proc. ICC'94* (New Orleans, LA, May 1994), pp. 650–654.
[12] D. Coulson, "The dual lattice of an extreme six-dimensional lattice," *J. Australian Math. Soc. (Ser. A)*, vol. 50, pp. 373–383, 1991.
[13] J. H. Conway and N. J. A. Sloane, "On the Voronoi regions of certain lattices," *SIAM J. Algebr. Discr. Meth.*, vol. 5, no. 3, pp. 294–305, Sept. 1984.
[14] R. T. Worley, "The Voronoi region of E_6^*," *J. Australian Math. Soc. (Ser. A)*, vol. 43, pp. 268–278, 1987.
[15] ——, "The Voronoi region of E_7^*," *SIAM J. Discr. Math.*, vol. 1, no. 1, pp. 134–141, Feb. 1988.
[16] T. J. Dickson, "The extreme coverings of 4-space by spheres," *J. Australian Math. Soc.*, vol. 7, pp. 490–496, 1967.
[17] E. S. Barnes and D. W. Trenerry, "A class of extreme lattice-coverings of n-space by spheres," *J. Australian Math. Soc.*, vol. 14, pp. 247–256, 1972.
[18] A. M. McLoughlin, "The complexity of computing the covering radius of a code," *IEEE Trans. Inform. Theory*, vol. IT-30, no. 5, pp. 800–804, 1984.